

Infrared Absorption Spectrum of Nitrous Oxide (N₂O) From 1830 cm⁻¹ to 2270 cm⁻¹*

Earle K. Plyler, Eugene D. Tidwell, and Arthur G. Maki

(August 9, 1963)

The frequencies of the vibration-rotation spectrum of N₂O have been measured from 1830 cm⁻¹ to 2270 cm⁻¹. A number of weak bands have been measured and assigned to "hot bands" and isotopic species in normal abundance. By using the Ritz principle and previously measured bands the bending frequency (ν_2) is calculated as 588.78₀ cm⁻¹. Frequencies are given for lines arising from the three principal transitions found in this region.

1. Introduction

Recently there has been considerable interest in obtaining accurate values for the vibration-rotation potential constants for small molecules. Pliva [1]¹ has measured the spectra of various isotopic species of nitrous oxide (N₂O) in the hope of obtaining more data with which to check the anharmonic terms of a potential function which he has devised [2]. Tidwell, Plyler, and Benedict [3] have reported measurements on a large number of vibrational-energy levels for N₂O and have derived a set of vibration-rotation constants.

Rank et al. [4] have reported the results of some very precise measurements on five absorption bands of N₂O. McCubbin, Grosso, and Mangus [5] have made some further precise measurements on N₂O which will be reported soon. While this work was in progress Fraley, Brim, and Rao [6] published results of measurements on the strongest absorption lines due to N₂O in the 5- μ region. The latter measurements are in essential agreement with those reported here.

2. Experimental Procedure

The spectra were measured on the NBS high-resolution infrared spectrometer described elsewhere [7]. Most of the measurements were made using a 7,500 lines/in. grating although some measurements were obtained with a 1,860 lines/in. grating. A liquid-nitrogen cooled PbSe detector was used. Calibration was achieved by the combination of accurately measured rare-gas spectra and a Fabry-Perot interferometer fringe system in the manner described in reference 8.

Spectra were obtained with pathlengths of 1.2, 4, and 24 m and pressures ranging from 1 to 200 mm Hg. Representative spectra are shown in figures 1 and 2. The 1.2 m cell could be either cooled to 220 °K or warmed to 400 °K; representative spectra obtained at these temperature extremes are shown in figures 3 and 4. In these figures it is evident that

many lines which are weak at low temperatures have intensified with increase in temperature. These lines must be attributed to transitions originating from excited vibrational states and accordingly have been assigned as "hot band" lines.

3. Analysis of Data

The microwave measurements of Burrus and Gordy [9] have given very precise values for the ground-state rotational constant, B_0 , and the l -doubling constant, q , of the molecule N¹⁴N¹⁴O¹⁶. Coles and Hughes [10] and Coles, Good, and Lide [11] have made further measurements from which one can obtain B_0 for the isotopes N¹⁴N¹⁵O¹⁶, N¹⁵N¹⁴O¹⁶, and N¹⁴N¹⁴O¹⁸. Combining the results of these workers with the velocity of light (taken as 299,793 km/s) we have calculated these constants in wave-numbers as given in table 1. Since these molecular constants are more accurate than could be obtained from the measurements reported here, the values given in table 1 were used wherever applicable for the calculation of the other molecular constants. For this same purpose the value of $D_0=17.6\times 10^{-8}$ cm⁻¹ given by Rank et al. [4] was used.

TABLE 1. Accurately known molecular constants used in the analysis of the N₂O bands between 4.4 and 5.5 μ

$B_{000}=0.419010_4$ cm ⁻¹
$D_{000}=17.6\times 10^{-8}$ cm ⁻¹
$q=79.17\times 10^{-5}$ cm ⁻¹
$B_{010}=0.419572_7$ cm ⁻¹ (average of c and d levels)
$B_{000}(\text{N}^{14}\text{N}^{15}\text{O}^{16})=0.418982_1$ cm ⁻¹
$B_{000}(\text{N}^{15}\text{N}^{14}\text{O}^{16})=0.404856_4$ cm ⁻¹
$B_{000}(\text{N}^{14}\text{N}^{14}\text{O}^{18})=0.39557_7$ cm ⁻¹

Since the data for many of the bands reported here was rather fragmentary due to the high degree of overlapping, all of the absorption bands were analyzed by obtaining a least-squares fit to the polynomial

$$\nu_{\text{obs}}=\nu_0+(B'+B'')m+(B'-B'')m^2-2(D'+D'')m^3-(D'-D'')m^4$$

where the terms have their usual significance.

*This work was supported in part by the Geophysics Research Directorate, Air Force Cambridge Research Laboratories.

¹ Figures in brackets indicate the literature references at the end of this paper.

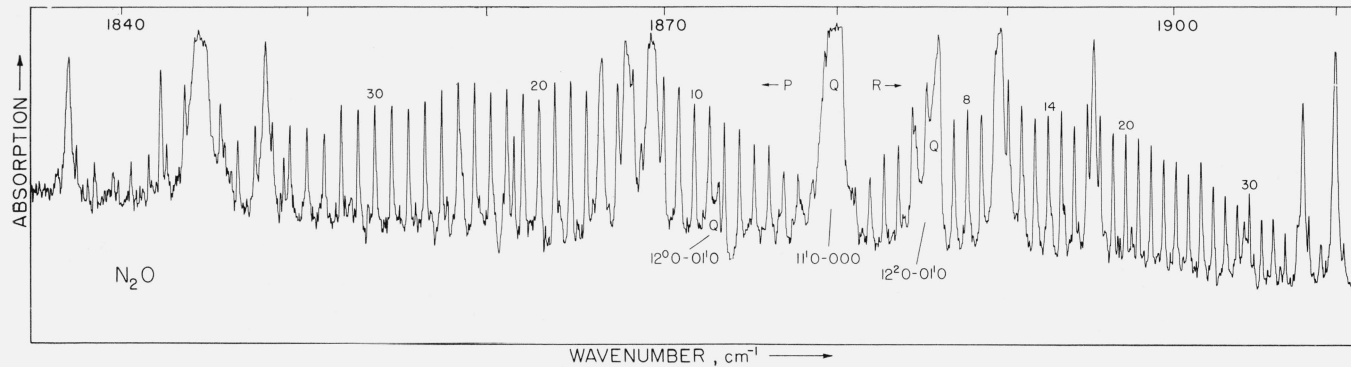


FIGURE 1. N₂O absorption from 1840 to 1910 cm⁻¹.

Pathlength 1.2 m; pressure 28 cm Hg.

08

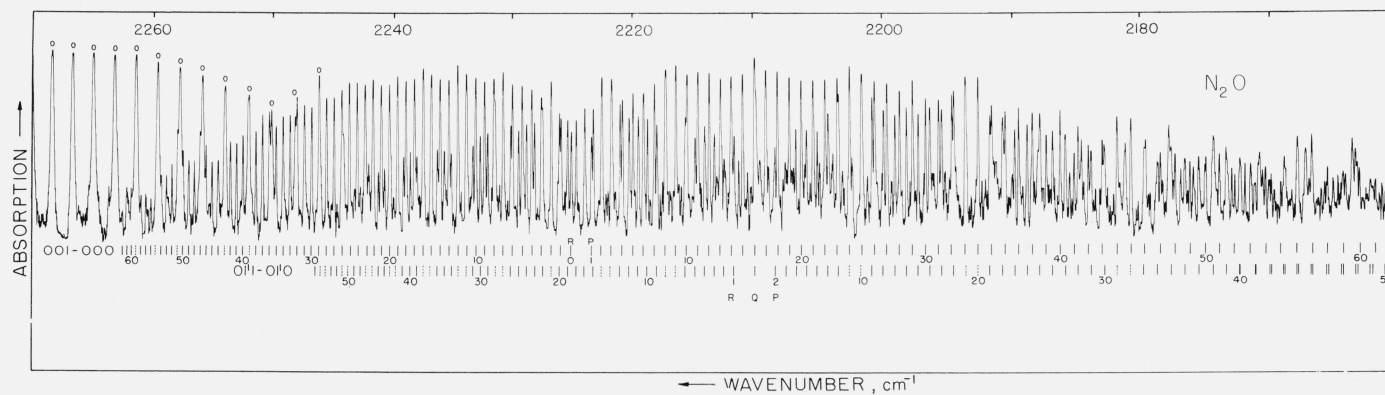


FIGURE 2. N₂O absorption from 2270 to 2160 cm⁻¹.

Pathlength 4 m; pressure 1 mm Hg. Circle: indicates absorption lines due to atmospheric C¹³O₂¹⁶ in the optical path.

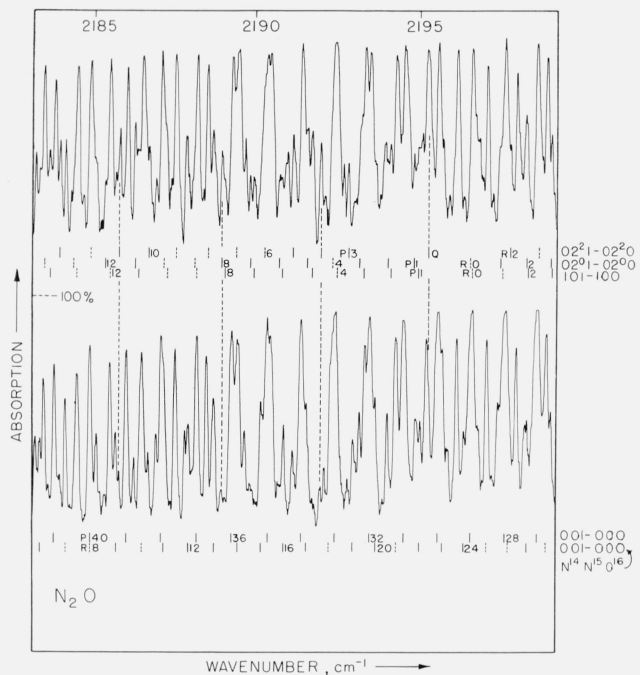


FIGURE 3. N_2O absorption from 2184 to 2200 cm^{-1} .

Upper curve is for a temperature of 400 °K and lower curve is with cell cooled to about 220 °K. Pathlength is 1.2 m; pressure 1 mm Hg.

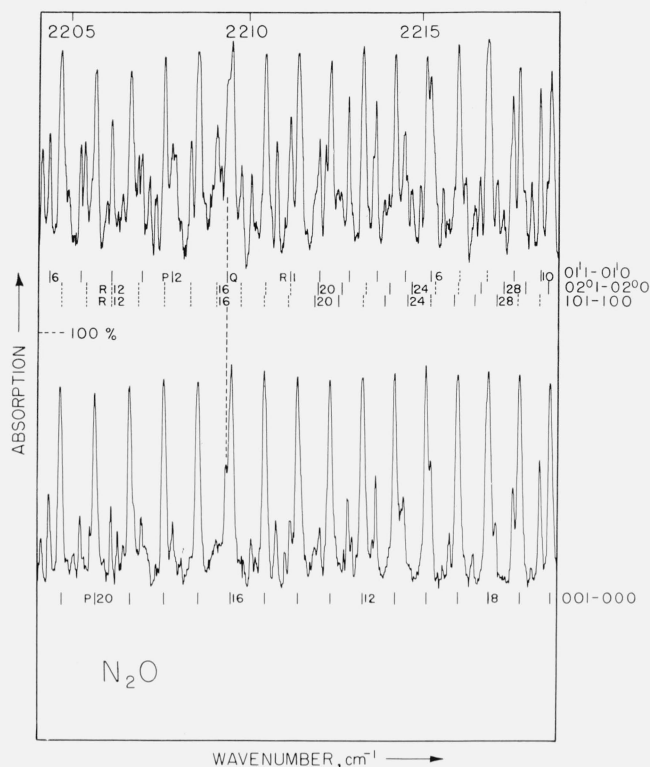


FIGURE 4. N_2O absorption from 2204 to 2220 cm^{-1} .

Temperature of gas in upper curve is 400 °K, temperature of gas in lower curve is 220 °K. Pathlength is 1.2 m; pressure is 2 mm Hg.

TABLE 2. Vibration-rotation constants describing the absorption bands of N_2O in the 2000 cm^{-1} Region

The limits of error given are standard deviations

Isotopic species	Assignment	ν_0	$\Delta B \times 10^{+5} cm^{-1}$	$*D' \times 10^8$	$*D'' \times 10^8$	$\Delta D \times 10^{+8}$
$N^{14}N^{14}O^{16}$	12 ⁰ –01 ^c 0	1873. 20 ₆ ± 0. 009	–9 ₃ ** ± 3	23. 8	17. 6	-----
	11 ¹ c0–000	1880. 271 ± . 003	–154. ₆ ± 0. 7	17. 6	17. 6	–0. 2 ± 0. 3
	12 ² c0–01 ¹ c0	} 1886. 03 ₃ ± . 009	–9 ₆ ± 3	{ 13. 1	} 17. 6	-----
	12 ² d0–01 ¹ d0					17. 6
	200–01 ¹ c0		1974. 571 ± . 003	–397. ₅ ± 1. 0	16. 1	17. 6
	200–01 ¹ d0	} 1988. 2 ± . 3 – Q branch position				
	21 ¹ 0–02 ² 0		1997. 6 ₃ ± . 15 – Q branch position			
	21 ¹ d0–02 ² 0					
	02 ² c1–02 ² c0	} 2195. 40 ₆ ± . 006	–340. ₃ ± 1. 2	{ 11. 6	} 11. 6	-----
	02 ² d1–02 ² d0					17. 6
	02 ² 1–02 ² 0	2195. 84 ₉ ± . 025	–336 ± 2	23. 6	23. 6	0 ± 1. 4
	101–100	2195. 9 ₃ ± . 04	–35 ₂ ± 5	17. 0	17. 4	-----
	01 ¹ 1–01 ¹ 0	2209. 52 ₇ ± . 004	–340. ₃ ± 0. 9	17. 6	17. 6	0. 4 ± 0. 3
	001–000	2223. 76 ₄ ± . 003	–345. 6 ± 0. 3	17. 4	17. 6	–0. 26 ± 0. 05
	$N^{14}N^{15}O^{16}$	01 ¹ 1–01 ¹ 0	2164. 13 ± . 03	–31 ₅ ± 15	17. 5	17. 5
001–000		2177. 659	–33 ₀ ± 3	17. 5	17. 5	-----
$N^{15}N^{14}O^{16}$	001–000	2201. 60 ₄ ± . 015	–33 ₇ ± 3	16. 5	16. 5	-----
$N^{14}N^{14}O^{18}$	001–000	2219. 67 ₈ ± . 02	–41 ₁ ± 10	16. 5	16. 5	-----

*In all cases the values of D given were assumed in order to obtain the best possible values of ν_0 , ΔB , and ΔD .

**This ΔB value is from the average of the c and d levels of the lower state.

The data were also analyzed using the method of combinations and differences. The results of both methods were comparable, but in many cases the fact that more lines could be used in fitting to the polynomial given above resulted in a reduction in the uncertainty of the various unknown constants when this method was used, especially since the lower state constants were in most cases very accurately known.

For those bands which are split into resolved *c* and *d* components the two bands were analyzed simultaneously to obtain a least-squares fit to the same band center and other constants were made compatible. A more detailed description is given for the individual bands in the next section.

4. Results

4.1. The Region From 1830 to 1925 cm^{-1}

In this region lines have been identified due to the three transitions $12^{00}-01^{10}$, $12^{20}-01^{10}$, and $11^{10}-000$. For all these perpendicular bands the *Q* branches were observed, but the resolution was not good enough to measure any individual *Q* branch lines. The splitting of the $\Delta-\Pi$ band was observed for all but a few low *J* lines. The analysis of this $\Delta-\Pi$ band was carried out by analyzing the *c* and *d* components simultaneously. Since the data were quite fragmentary for these weak "hot bands," the best available estimates of the values of B'_c , B'_d , D'_c , and D'_d were used in order to obtain more accurate values of ν_0 and B' . For this purpose it was assumed that $B'_c=B'_d$. Since the *c* and *d* levels of the 12^{20} state undergo *l*-type resonance with different levels, it was necessary to use different values of *D* for the *c* and *d* levels. The values of the constants used are given in table 2. Only the *c* component of the $\nu_1+\nu_2$ band was measured, therefore the value obtained for ΔB as given in table 2 is for the transition to the *c* level only.

The calculated and observed frequencies of absorption lines due to the transition $11^{10}-000$ are given in table 3. Figure 1 shows the appearance of the absorption in this region.

4.2. Absorption Lines in the Region 1925 to 2000 cm^{-1}

The main band found in this region is a $\Sigma-\Pi$ band due to the transition $200-01^{10}$. In this case the *Q* branch was sufficiently well resolved so that measurements were obtained for both the *c* and *d* levels. Since microwave values for the lower state are quite good, these values were used in the analysis and transitions from both the *c* and *d* levels were analyzed simultaneously by a least-squares program in order to obtain the best values for ν_0 and B' .

Absorption in this region was very weak as might be expected from the transitions involved. The *Q* branches for the two "hot bands" $21^{10}-02^{20}$ and $21^{10}-02^{00}$ were also observed in this wavelength

region, but they were not resolved. Nor were any lines of the *P* and *R* branches observed.

The calculated and observed frequencies of the lines for the $200-01^{10}$ transition are given in table 3.

4.3. $\text{N}^{14}\text{N}^{14}\text{O}^{16}$ Absorption Between 2130 and 2270 cm^{-1}

The fundamental ν_3 and associated "hot bands" are located in this region. ν_3 is a rather strong absorption band, consequently with the pathlength and resolution available it was possible to obtain measurements on four "hot bands" and four isotopic bands.

The splitting of the first "hot band" was observed for high-*J* levels but overlapping with various other bands was rather severe. For this reason it was felt that more accurate band constants could be obtained by averaging the frequencies of the *c* and *d* components. Even though this procedure did not permit the use of measurements where only one component was observed, the resultant constants are believed to be more reliable than those found by analyzing each band individually.

Lines due to the $\Delta-\Delta$ transition $02^{21}-02^{20}$ have been observed and the position of the *Q*, while overlapped, has been verified by observations at 220 °K and 400 °K. Figure 3 shows a few lines due to this transition and the manner in which the line intensities change with temperature. The Boltzman distribution predicts this transition will show an approximate six-fold increase in intensity in going from 220 °K to 400 °K.

Since the two $\Sigma-\Sigma$ transitions $101-100$ and $02^{01}-02^{00}$ are predicted to lie quite close to each other, some difficulty was anticipated in assigning the two series of lines which must be due to these transitions. The assignments of these lines are, however, considered to be reliable due to the rather large differences in the lower-state *B* values. $\Delta_2\bar{F}''$ plots for these two bands yield respective B'' values of 0.4175 and 0.4200 cm^{-1} . The B'' values expected from the data of reference 3 are 0.41725 and 0.41991, respectively. Many of the low-*J* lines are badly overlapped because the two band centers lie so close together. As a consequence the band centers calculated from the data may be in error by several hundredths of a wavenumber. The statistical treatment of the data resulted in a standard deviation for the ν_0 values of 0.01 cm^{-1} , but inspection of the data leads us to believe that this is not a realistic number. Therefore table 2 contains a more subjective evaluation of the accuracy of the band centers for these two bands.

Table 4 lists the frequencies of the ν_3 band as observed in this laboratory and as reported by Fraley, Brim, and Rao. Columns 3 and 6 compare the calculated frequencies with those observed.

4.4. Isotopic Absorption Bands From 2100 to 2240 cm^{-1}

Within this region absorption bands due to N_2O molecules containing N^{15} or O^{18} are expected. Lines

TABLE 3. Observed and calculated wavenumbers for the two strongest N₂O absorption bands between 1830 and 2000 cm⁻¹

J''	11 ^{1c} 0-000				200-01 ^{1c} 0				200-01 ^{1d} 0	
	P		R		P		R		Q	
	Obs.	Calc.	Obs.	Calc.	Obs.	Calc.	Obs.	Calc.	Obs.	Calc.
0			1881.095	.106						
1			81.929	.937			^b 1976.222	.227		
2	^b 1878.595	.591	82.751	.766						
3	^b 77.766	.747	83.600	.592			^b 77.832	.853		
4	76.894	.900					^b 78.643	.656		
5	76.041	.050								
6	75.185	.196					^b 80.253	.239		
7			86.865	.863			81.016	.020		
8	^b 73.472	.480					81.790	.794		
9					^b 1966.764	.769	82.559	.561		
10					^b 65.880	.867	83.317	.320		
11					64.952	.957	84.081	.073	1973.995	.995
12			^b 90.861	.882	64.034	.040	84.821	.818		
13			^b 91.684	.677	63.127	.117	85.553	.556	73.784	.777
14			^b 92.488	.468	62.181	.186	86.287	.287	73.636	.655
15			93.253	.256			87.030	.010	73.543	.524
16			94.054	.041	60.302	.303	87.723	.727	73.400	.384
17	^b 65.590	.607	^b 94.850	.823	59.351	.351			73.218	.236
18	^b 64.720	.717	^b 95.585	.601	58.399	.392	89.127	.139	73.088	.079
19	^b 63.844	.824			57.422	.426	89.833	.834	72.920	.914
20	^b 62.958	.928	97.150	.149	56.448	.453	90.521	.522	72.754	.740
21			97.910	.918	55.465	.473			72.560	.557
22	61.130	.128	98.674	.684	54.494	.489			72.381	.366
23	60.210	.223	1899.436	.447	53.490	.493			72.160	.166
24	59.315	.315	^b 1900.190	.207	52.487	.492	93.222	.202	^b 71.986	.957
25			00.964	.963	51.481	.484	93.859	.855	71.746	.740
26	57.496	.491	01.715	.716	50.469	.470	94.496	.500	71.518	.514
27	56.576	.574	^b 02.493	.466	^b 49.440	.449	95.138	.138	^b 71.258	.280
28	55.662	.654	03.221	.213	48.423	.420	95.777	.770	^b 71.032	.037
29	54.739	.732	03.960	.957	47.383	.386	96.389	.394	70.787	.786
30	53.808	.806	04.689	.697					70.518	.526
31	52.884	.877	05.425	.435			^b 97.600	.621	^b 70.270	.258
32	51.950	.946	06.154	.169	44.234	.240	^b 1998.197	.224	69.987	.981
33	51.012	.012	06.883	.900	^b 43.171	.178			1969.700	.696
34	50.062	.074	^b 07.617	.627						
35	49.125	.134	08.348	.352	41.034	.033				
36			09.070	.073	39.938	.951				
37	^b 47.256	.245			38.880	.862				
38	^b 46.266	.296	10.517	.506	^b 37.783	.767				
39			11.220	.217	36.680	.665				
40			11.931	.926	35.542	.556				
41			12.626	.631	1934.443	.441				
42	^b 42.475	.472	13.345	.333						
43	41.518	.509	14.024	.032						
44	40.544	.543	^b 14.720	.727						
45	^b 39.591	.574	1915.421	.420						
46	38.604	.602								
47										
48	36.662	.650								
49	35.672	.670								
50	34.696	.687								
51	33.700	.701								
52	32.712	.712								
53	^b 1831.720	.721								

^b Blended or weak lines.

TABLE 4. Wavenumbers of absorption lines for the ν_1 band of N_2O

J	P Branch			R Branch		
	Observed wave-number NBS	Calc. NBS	Observed wave-number ref. 6	Observed wave-number NBS	Calc. NBS	Observed wave-number ref. 6
0				2224. 59 ₃	2224. 59 ₅	2224. 59 ₄
1	^b 2222. 90 ₀	2222. 92 ₆	2222. 94 ₀	^b 25. 41 ₁	25. 41 ₆	25. 43 ₀
2	^b 22. 06 ₅	22. 08 ₁	22. 08 ₅	^b 26. 23 ₇	26. 23 ₆	26. 24 ₃
3	^b 21. 25 ₃	21. 22 ₉	21. 27 ₃	(^b)		27. 05 ₀
4	20. 36 ₁	20. 37 ₀	20. 38 ₂	27. 84 ₅	27. 85 ₀	27. 84 ₈
5	19. 51 ₄	19. 50 ₅	19. 51 ₆	28. 65 ₀	28. 64 ₇	28. 63 ₉
6	18. 63 ₈	18. 63 ₂	18. 64 ₁	^b 29. 45 ₉	29. 43 ₆	29. 45 ₀
7	17. 74 ₅	17. 75 ₃	17. 75 ₆	^b 30. 22 ₄	30. 21 ₉	30. 21 ₈
8	^b 16. 83 ₃	16. 86 ₇	16. 84 ₀	^b 30. 97 ₅	30. 99 ₅	30. 97 ₅
9	^b 15. 97 ₅	15. 97 ₃	15. 98 ₃	31. 78 ₄	31. 76 ₃	31. 74 ₁
10	^b 15. 10 ₉	15. 07 ₃	15. 08 ₈	32. 54 ₃	32. 52 ₅	32. 54 ₈
11	14. 17 ₅	14. 16 ₆	14. 17 ₃	(^b)		33. 30 ₁
12	13. 24 ₄	13. 25 ₃	13. 26 ₉	^b 34. 02 ₁	34. 02 ₈	34. 02 ₃
13	12. 30 ₄	12. 33 ₂	12. 33 ₀	34. 78 ₄	34. 76 ₀	34. 80 ₆
14	11. 40 ₄	11. 40 ₅	11. 42 ₀	35. 52 ₆	35. 50 ₃	35. 50 ₉
15	^b 10. 46 ₉	10. 47 ₀	10. 47 ₈	^b 36. 25 ₃	36. 22 ₀	36. 24 ₆
16	(^b)		09. 52 ₃	^b 36. 94 ₂	36. 95 ₀	36. 94 ₇
17	^b 08. 58 ₂	08. 58 ₁	08. 59 ₀	^b 37. 67 ₀	37. 66 ₃	37. 66 ₃
18	09. 62 ₅	07. 62 ₆	07. 62 ₂	38. 36 ₄	38. 36 ₉	38. 36 ₈
19	06. 66 ₉	06. 66 ₅	06. 66 ₈	^b 39. 07 _e	39. 06 ₈	39. 07 ₆
20	05. 68 ₁	05. 69 ₆	05. 68 ₇	^b 39. 72 _s	39. 76 ₀	39. 76 ₁
21	04. 71 ₉	04. 72 ₁	04. 71 ₇	40. 45 ₄	40. 44 ₅	40. 44 ₄
22	^b 03. 73 ₇	03. 73 ₉	03. 73 ₅	41. 13 ₁	41. 12 ₃	41. 13 ₀
23	^b 02. 73 ₆	02. 75 ₀	02. 74 ₁	41. 78 ₀	41. 79 ₄	41. 80 ₅
24	^b 2201. 74 ₇	2201. 75 ₄	01. 75 ₂	42. 46 ₆	42. 45 ₈	42. 44 ₃
25			2200. 77 ₂	43. 12 ₅	43. 11 ₅	43. 12 ₀
26	2199. 72 ₀	2199. 74 ₂	2199. 73 ₅	43. 75 ₉	43. 76 ₅	43. 77 ₃
27	98. 72 ₆	98. 72 ₆	98. 73 ₅	44. 42 ₁	44. 40 ₉	44. 41 _e
28	97. 70 ₇	97. 70 ₄	97. 69 ₆	45. 04 ₃	45. 04 ₅	45. 04 ₉
29	96. 67 ₇	96. 67 ₄	96. 66 ₇	^b 45. 66 _s	45. 67 ₄	45. 68 ₈
30	95. 64 ₅	95. 63 ₈	95. 63 ₁			46. 28 ₉
31	94. 60 ₉	94. 59 ₄	94. 60 ₂	46. 89 ₅	46. 91 ₁	46. 91 ₈
32	^b 93. 52 ₆	93. 54 ₅	93. 52 ₈	47. 53 ₁	47. 51 ₉	47. 50 ₉
33	(^b)		92. 42 ₈	48. 11 ₄	48. 12 ₀	48. 11 ₉
34	^b 91. 43 ₂	91. 42 ₅	91. 43 ₃	48. 71 ₂	48. 71 ₄	48. 71 ₄
35	^b 90. 34 ₅	90. 35 ₅	90. 34 ₉	49. 30 ₄	49. 30 ₁	49. 32 ₈
36	89. 26 ₄	89. 27 ₈	89. 28 ₀	49. 88 ₇	49. 88 ₁	49. 88 ₉
37	88. 18 ₄	88. 19 ₄	88. 18 ₉	50. 46 ₀	50. 45 ₄	50. 44 ₉
38	87. 13 ₁	87. 10 ₄	87. 10 ₆	51. 03 ₃	51. 02 ₀	51. 04 ₇
39	86. 00 ₂	86. 00 ₇	86. 00 ₄	(^b)		
40	84. 91 ₁	84. 90 ₃	84. 89 ₀	52. 14 ₅	52. 13 ₁	52. 14 ₈
41	83. 79 ₄	83. 79 ₃	83. 79 ₀	52. 68 ₂	52. 67 ₆	52. 68 ₅
42	82. 66 ₆	82. 67 ₆	82. 66 ₇	53. 20 ₉	53. 21 ₄	53. 21 ₆
43	^b 81. 56 ₀	81. 55 ₂	81. 54 ₅	(^b)		
44	(^b)		80. 38 ₀	54. 23 ₆	54. 26 ₈	54. 25 ₃
45	^b 79. 30 ₃	79. 28 ₅	79. 29 ₃	54. 79 ₆	54. 78 ₅	2254. 79 ₉
46	(^b)		78. 14 ₂	55. 31 ₈	55. 29 ₅	
47	76. 98 ₂	76. 99 ₁	76. 98 ₃	55. 79 ₆	55. 79 ₇	
48	75. 84 ₀	75. 83 ₄	75. 83 ₈	56. 28 ₇	56. 29 ₃	
49	74. 67 ₄	74. 67 ₀	74. 67 ₂	56. 76 ₂	56. 78 ₁	
50	73. 49 ₇	73. 50 ₀	73. 48 ₈	^b 57. 30 ₀	57. 26 ₃	
51			72. 32 ₄	^b 57. 70 ₇	57. 73 ₇	
52	71. 14 ₄	71. 13 ₉	71. 13 ₄	58. 21 ₃	58. 20 ₅	
53	^b 69. 89 ₈		69. 89 ₁	58. 66 ₄	58. 66 ₅	
54	68. 75 ₁	68. 75 ₂	68. 75 ₉	59. 13 ₁	59. 11 ₉	

See note at end of table.

TABLE 4. Wavenumbers of absorption lines for the ν_1 band of N_2O —Continued

J	P Branch			R Branch		
	Observed wave-number NBS	Calc. NBS	Observed wave-number ref. 6	Observed wave-number NBS	Calc. NBS	Observed wave-number ref. 6
55	67. 53 ₈	67. 54 ₉	2167. 57 ₉	(^b)		-----
56	^b 66. 31 ₈	66. 33 ₉	-----	60. 00 ₁	60. 00 ₄	-----
57	(^b)	-----	-----	60. 41 ₉	60. 43 ₆	-----
58	63. 92 ₆	63. 90 ₀	-----	60. 88 ₂	60. 86 ₂	-----
59	62. 69 ₀	62. 67 ₀	-----	^b 61. 28	61. 28 ₀	-----
60	61. 41 ₈	61. 43 ₄	-----	61. 67 ₅	61. 69 ₁	-----
61	60. 21 ₀	60. 19 ₁	-----	62. 08 ₂	62. 09 ₅	-----
62	58. 97 ₉	-----	-----	62. 48 ₉	62. 49 ₂	-----
63	57. 69 ₃	57. 68 ₆	-----	(^b)	-----	-----
64	56. 42 ₂	56. 42 ₄	-----	-----	-----	-----
65	55. 16 ₈	55. 15 ₅	-----	63. 63 ₆	63. 64 ₀	-----
66	53. 88 ₃	53. 88 ₀	-----	64. 02 ₀	64. 00 ₉	-----
67	-----	-----	-----	64. 36 ₂	64. 37 ₁	-----
68	51. 29 ₅	51. 31 ₀	-----	64. 74 ₁	64. 72 ₅	-----
69	^b 49. 97 ₆	50. 01 ₅	-----	(^b)	-----	-----
70	48. 74 ₀	48. 71 ₄	-----	65. 42 ₉	65. 41 ₄	-----
71	47. 36 ₉	47. 40 ₆	-----	(^b)	-----	-----
72	46. 09 ₇	46. 09 ₂	-----	^b 66. 08	66. 07 ₄	-----
73	44. 73 ₆	44. 77 ₁	-----	^b 66. 40	66. 39 ₃	-----
74	^b 43. 46	43. 44 ₄	-----	^b 66. 71 ₃	66. 70 ₅	-----
75	(^b)	-----	-----	(^b)	-----	-----
76	(^b)	-----	-----	(^b)	-----	-----
77	^b 39. 43 ₈	39. 42 ₄	-----	^b 2267. 61 ₂	2267. 60 ₀	-----
78	^b 2138. 08 ₆	2138. 07 ₂	-----	-----	-----	-----

^b Blended or weak lines.

due to four transitions in such isotopically substituted molecules have been identified in this study.

The band at 2201.60 cm^{-1} due to $N^{15}N^{14}O^{16}$ has been previously measured by Pliva [1] but bands due to the molecules $N^{14}N^{15}O^{16}$ and $N^{14}N^{14}O^{18}$ found at 2164.13, 2177.66, and 2219.67 cm^{-1} have not been previously reported. The assignments for these latter three bands have been confirmed by determination of the values of B'' from the $\Delta_2 F''$ plots. In the case of the $\Pi-\Pi$ transition at 2164.13 cm^{-1} the sharp Q branch seems to be observable at 2164.128 cm^{-1} , thus providing greater confidence in the position of the band center. Since many of the lines for these isotopic molecules were weaker than or of comparable intensity with the "hot bands" of the most abundant molecule, the identification of the lines was greatly aided by spectra obtained at 220 °K. At this temperature the intensity of the "hot band" lines is very greatly diminished. This leaves the isotopic lines as the most outstanding of the weak lines at low temperatures.

4.5. Discussion of Results

By means of the Ritz principle the position of some of the low-lying vibrational levels may be obtained. The bending vibration, ν_2 , may be obtained in four different ways. Using the precise measurements of reference 4 and the recent measurements of reference 5, we find

$$\begin{aligned} \nu_2^1 &= (12^0-000) - (12^0-01^10) \\ &= 2461.998 - 1873.206 = 588.792 \text{ cm}^{-1} \end{aligned}$$

$$\begin{aligned} \nu_2^1 &= (200-000) - (200-01^10) \\ &= 2563.341 - 1974.571 = 588.770 \text{ cm}^{-1} \end{aligned}$$

$$\begin{aligned} \nu_2^1 &= (11^10-000) - (11^10-01^10) \\ &= 1880.271 - 1291.496 = 588.775 \text{ cm}^{-1} \end{aligned}$$

Taking the average of the values given for the 01¹–000 transition in references 1 and 3, one obtains

$$\begin{aligned} \nu_2^1 &= (01^11-000) - (01^11-01^10) \\ &= 2798.308 - 2209.527 = 588.781 \text{ cm}^{-1}. \end{aligned}$$

TABLE 5. Comparison of the results of measurements on N_2O in different laboratories

	001-000		01 ¹ 1-01 ¹ 0		001-000 N ¹⁵ N ¹⁴ O ¹⁶	
	ν_0	$\Delta B \times 10^5$	ν_0	$\Delta B \times 10^5$	ν_0	$\Delta B \times 10^5$
	NBS (this work)-----	2223.764	-345.6	2209.527	-340.3	2201.604
Pliva (ref. 1)-----	2223.754	-344.7	2209.521	-341.2	2201.605	-336.0
Fraley, Brim, and Rao (ref. 6)-----	2223.759	-344.6	2209.535	-----	-----	-----

The average of these four indirect determinations, 588.780 cm^{-1} , compares very favorably with the indirect measurement of Pliva [1] (588.767 cm^{-1}), the four indirect measurements of Tidwell et al. [3] (588.773 cm^{-1}), and the direct measurement of Lakshmi, Rao, and Nielsen [12] (588.78 cm^{-1}).

The Ritz principle may also be applied to determine the values of $2\nu_2^0$, $2\nu_2^2$, and ν_1 as follows:

$$\begin{aligned}
 2\nu_2^2 &= (02^21-000) - (02^21-02^20) \\
 &= 3373.184 - 2195.406 = 1177.778 \text{ cm}^{-1} \\
 2\nu_2^0 &= (02^01-000) - (02^01-02^00) \\
 &= 3363.997 - 2195.85 = 1168.15 \text{ cm}^{-1} \\
 \nu_1 &= (101-000) - (101-100) \\
 &= 3480.854 - 2195.93 = 1284.92 \text{ cm}^{-1}
 \end{aligned}$$

where the values for the vibration levels given by Pliva [1] and Tidwell et al. [3] are used. By using similar combinations Tidwell et al., have previously determined $2\nu_2^2 = 1177.78 \text{ cm}^{-1}$. McCubbin et al. [5] have recently measured $2\nu_2^0$ and ν_1 at 1168.13_4 and $1284.90_7 \text{ cm}^{-1}$, respectively. These were direct measurements and should be more accurate than the indirectly obtained values given above.

The band centers for the transitions 001-000 and 01¹1-01¹0 have now been measured quite carefully in three different laboratories. Some idea of the absolute accuracy of these measurements may be obtained by comparing the constants derived from the measurements. We may also compare the measurements of ν_3 for the N¹⁵N¹⁴O¹⁶ molecule with those reported by Pliva [1]. Table 5 shows how closely these independent measurements agree. Although it is seen that Pliva and Fraley et al., agree on a slightly larger value for B_{001} than has been reported in this work, nevertheless it is felt that the values given here are probably more accurate. The present measurements extend to considerably higher values of J than previous measurements and as a conse-

quence a more accurate determination of ΔB and ΔD is expected. On the other hand Fraley, Brim, and Rao probably have a more accurate value for ν_0 since their resolution was slightly better so that blending of low- J lines would have less tendency to cause errors in the derived ν_0 . Since Pliva worked with an isotopically enriched sample, it is to be expected that his constants for N¹⁵N¹⁴O¹⁶ are better than those reported here.

An attempt was made to compare the results of this work with the constants given by Tidwell et al., but, as noted by Pliva [1], the agreement is not entirely satisfactory. Perhaps the measurements given here will be of value in determining the accuracy of the revised constants which Pliva is calculating.

5. References

- [1] Josef Pliva, International Symposium on Molecular Structure and Spectroscopy, Sept. 1962, Tokyo, Japan.
- [2] Josef Pliva, Collection Czech. Chem. Commun. **23**, 777 (1958).
- [3] E. D. Tidwell, E. K. Plyler, and W. S. Benedict, J. Opt. Soc. Am. **50**, 1243 (1960).
- [4] D. H. Rank, D. P. Eastman, B. S. Rao, and T. A. Wiggins, J. Opt. Soc. Am. **51**, 929 (1961).
- [5] T. K. McCubbin, R. Grosso, and J. Mangus, to be published.
- [6] P. E. Fraley, W. W. Brim, and K. N. Rao, J. Mol. Spect. **9**, 487 (1962).
- [7] E. K. Plyler and L. R. Blaine, J. Res. NBS **62**, (Phys. and Chem.) No. 1,7 (1959).
- [8] E. K. Plyler, L. R. Blaine, and E. D. Tidwell, J. Res. NBS **55**, 279 (1955) RP2630.
- [9] C. A. Burrus and W. Gordy, Phys. Rev. **101**, 599 (1956).
- [10] D. K. Coles and R. H. Hughes, Phys. Rev. **76**, 178A (1949).
- [11] P. Kislink and C. H. Townes, NBS Circ. 518 (1952).
- [12] K. Lakshmi, K. N. Rao, and H. H. Nielsen, J. Chem. Phys. **24**, 811 (1956).

(Paper 68A1-255)